Mechanical Surface Treatment of Polymer Parts Produced by FFF

S. Dietrich*, B. Karcher†, U. Popp† and J. Scholz†

* Institute for Applied Materials – Materials Science and Engineering, Karlsruhe Institute of Technology,
Karlsruhe 76131, Germany
†Apium Additive Technologies GmbH, 76187 Karlsruhe, Germany

Abstract

The surface structure in the form of waviness and roughness as well as near surface density of FFF parts represents a major issue with respect to mechanical performance especially under fatigue loading. Mechanical surface treatments like shot peening or rolling are commonly used techniques, especially for metal components, to reduce surface roughness, increase surface densification and create beneficial residual stress states in the surface layer. In this study, a rolling process has been applied intermittently with the layer-wise FFF process and the effect on the surface state has been investigated using laser scanning and optical microscopy as well as micro-computed tomography. A process window with different rolling tools and rolling paths has been identified and analysed. The results show clearly advantageous properties regarding an improved surface roughness, with a higher densification gradient in the first perimeter tracks of the FFF extrusion strategy as well as sharper corners being realized.

Introduction

Material extrusion or fused filament fabrication (FFF) is an additive manufacturing process that can be used to process both amorphous and semi-crystalline thermoplastics. In addition to standard and engineering plastics such as acrylonitrile butadiene styrene (ABS) or polycarbonate (PC), this also includes high-performance polymers such as Polyetheretherketone (PEEK) which are often applied in fields with high static and fatigue loads. During the process, the plastic filament is fed by the extruder, in the direction of the print head. Part of the print head is a heated nozzle in which the filament is melted and extruded through the nozzle opening with a diameter of usually 0.2 to 0.8 mm. The polymer then solidifies along the machine-controlled path on the build platform and forms the cross sections of the component to be produced. Due to this characteristic strand by strand and layer wise deposition process the surface quality and also the microstructure of the boundary layer show a reduced precision and an increase in defect density respectively. This work aims at developing a hybrid FFF process with integrated surface finishing. A rolling tool in replacing the secondary print head enables CNC control and three-dimensional movement using conventional Gcode. The hybrid process enables forming and chipless surface finishing by local re-melting and smoothing.

State of the Art

The surface and boundary layer properties of FFF parts are mainly influenced by the processing parameters including the layer thickness, the extrusion strategy (raster angle, air gap and build orientation) and the nozzle size. Due to the predefined layer thickness, the vertical resolution is limited. Printed components show clearly visible layer lines and staircase effects. A lower layer height results in a finer vertical resolution, which minimizes the effects mentioned. Consequently, however, more layers have to be deposited, which increases the printing time. The creation of internal defects is mainly controlled by the extrusion path with characteristic triangular gaps when the hatching strands joins the perimeter strand under different angles in a cross section. These pores additionally contribute to an overall degradation of the mechanical properties besides the surface roughness stemming from the essentially circular strand cross section in the outer perimeter [1]. Experiments in [2] showed that doubling the layer height from 0.1 to 0.2 mm resulted in a drop in tensile strength of 6 to 11 percent. For this purpose, tensile specimens were produced and tested according to ASTM D638-14 by means of material extrusion from the materials ABS and polylactic acid (PLA). Similar correlations between tensile strength and layer height were found in [3, 4]. In [5] the mechanism of strength reduction was based on a lower porosity as a result of smaller layer heights, as investigated by means of optical microscopy. With regard to high strength polymers the investigations of PEEK tensile specimens in [6] determined a layer height of 0.3 mm to result in a maximum tensile strength. Rajpurohit and Dave name internal pores as sites of origin for cracks and crack growth [7].

The review in [8] of different surface finishing processes clearly identifies the surface roughness, caused by the layered structure, as responsible for crack growth in investigations of FFF samples [8]. In addition to reducing visible layer lines and staircase effects as relevant roughness mechanisms, a surface that is as free of defects as possible further reduces the formation of cracks and notch effects. Furthermore, post-processing of the surface can have a targeted influence on the dimensional accuracy of functional surfaces.

The classifications of surface finishing processes for printed parts in [8-10] divide existing processes into mechanical and chemical processes with an additional extension through thermal and hybrid processes.

Mechanical processes are based on the principle of cutting or forming the tips of surface profiles. Grinding uses geometrically indeterminate cutting edges of various sizes [11]. Turning and milling processes, on the other hand, can be automated or manually controlled. In this case, the geometrically determined cutting edge is guided by a machine and all points of a component that can be reached without collision can be machined. However, the workpiece must be fixed in a clamping device, which can damage its surface [11]. Compressed air blasting with a solid abrasive or shot peening are processes that can be used to reach even hard-to-reach points on a component. In these processes, an abrasive or shot is accelerated by compressed air onto the surface of the workpiece. Depending on the abrasive used and the process parameters, the effect of this process can be influenced. While sand has an abrasive effect, the use of metal beads reshapes the tips of the surface profiles [8,12]. Compared to the processes already mentioned, vibratory finishing enables the simultaneous machining of several components. For this purpose, these are placed in a rotating work container together with grinding wheels. The size and geometry of the grinding tools used ultimately determine whether all areas of the workpieces can be machined [13]. Rolling or burnishing is another tool-based process that can be carried out on a CNC-machine with an average reduction in surface roughness by 70%. A slight but significant improvement in mechanical performance can be seen in the higher impact absorption energy and the longer fatigue life which are attributed to surface hardening and compressive residual stresses introduced by this mechanical surface treatment [14].

Printed ABS components can be chemically reworked by bathing them in acetone or acetone vapour. Acetone is a colourless, low-cost liquid with high diffusion and a boiling temperature of 56 °C. Due to these properties and its low toxicity, this solvent is preferred for ABS, along with others such as esters and chlorides, for surface finishing [15]. The liquid acetone or its vapour reaches places that cannot be reached by mechanical methods. Similarly, no clamping is necessary (cf. section 2.4.1). However, if the component remains exposed to the acetone for too long, there is a risk that it will deform in its entirety and fine details will be lost [15].

Thermal methods use externally applied thermal energy to locally smooth the surface [8]. Laser-based methods, such as laser re-melting (LR), create a localised zone of molten material. Due to the surface tension of the melt, a smoothed surface remains after solidification. With this non-contact process, all surfaces that can be reached by the laser can be smoothed [16].

Overall, the role of mechanical surface treatments in FFF can mainly be seen in the contribution to a smoother surface and better tolerances of the parts [17].

Experimental Setup

For the mechanical surface treatment experiments carbon fiber reinforced Polyetheretherketon Apium (PEEK CFR 4000) with a fiber volume fraction of 30 % was used since this is a high-performance polymer where the expected potential for mechanical improvement is expected to be the highest. The printing process was carried out with the parameters depicted in Table 1 on a Apium P400 with a temperature of the extrusion head of 510 °C by the co-authors from Apium Additive Technologies GmbH.

Table 1: Printing parameters used in the PrusaSlicer v2.5.0 for the manufacturing of the test cubes.

Process parameter	Value
Nozzle diameter	0.4 mm
Layer height	0.3 mm
Track width	0.48 mm
Velocity in the perimeter	15 mm/s
Velocity in the hatching	30 mm/s

An adaptive zone heater enables near isotropic part characteristics while being more energy efficient than conventional build space heaters. Furthermore, the Apium P400 offers two printhead mounts on the Y-axis which can be independently moved along the X-axis for independent dual extrusion. In this work one print head is replaced by the developed surface finishing tool described in the results section (see Figure 1).

As sample geometries cubes with an edge length of 20 mm were manufactured and post processed with different surface treatment parameters. The cubes were built as hollow structures with diagonal supports (hatching with a fill factor of 6 %) and walls made of three perimeter tracks.
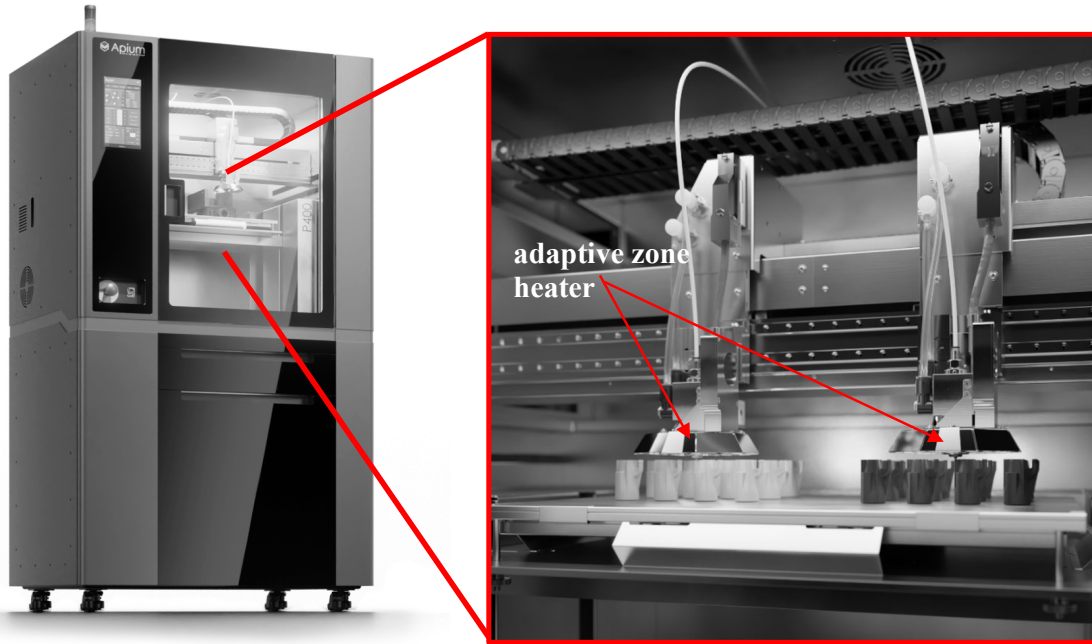
Figure 2: Apium P400 dual extrusion printer (left) with a close up of the build space showing two extrusion heads with the adaptive zone heater (right).

A Y.CT Precision microfocus system from Yxlon was used to carry out the Micro-CT measurements. The built-in area detector enabled images in the size 2048 x 2048 pixels. The pixels of the two-dimensional projections and the voxels of the three-dimensional reconstructions had an isotropic edge length of 16 µm. The VGStudio Max software from Volume Graphics was used to reconstruct the CT images. Subsequently, sectional views were created and the density gradients were analysed using the open-source software package Fiji. A µsurf confocal microscope from Nanofocus was used to analyse the surface roughness. During the measurements, an area of the component surface was recorded and any tilting of the samples relative to the lens was removed by calculation. The roughness analysis was carried out according to DIN EN ISO 4287. Light optical microscope images were taken with a Zeiss microscope. By varying the focus, several individual images with different focal points were superimposed, resulting in high-resolution images with 50x and 100x magnification, even with a rough surface.

Results and Discussion

Tool Design

In order to develop the mechanical surface treatment tool in a first step geometrical considerations of the necessary plastic deformation to flatten the surface layer were carried out in order to predict the necessary tool infeed. Using the simplified layer geometry in Figure 2 left with a layer height h = 2r a relation between the necessary radial infeed v and the layer height can be derived as:

$$v = h\left(\frac{1}{2} - \frac{\pi}{8}\right)$$

With the help of this equation, the optimal radial infeed of the burnishing tool with a layer height of h=0.3 mm is calculated as v≈0.03 mm. As another processing parameter, the relative forming layer height describes the ratio of absolute forming and printing layer height. These values were used to program the tool path instructions with the parameters depicted in Figure 2 right. For this purpose, a software was created in Blender and integrated into the controls of the Apium P400 which consists of four main modules. First, the STL file of the component and the associated Gcode are imported. The component is then divided into layers for forming, whereby the forming layer height can be selected independently of the print layer height. Path generation is done by expanding the outer contour of the layers by a predefined distance. Collision checks ensure that features that cannot be mapped geometrically are avoided. The radial distance of the forming tool to the part and the axial engagement are defined to ensure contact and safety.
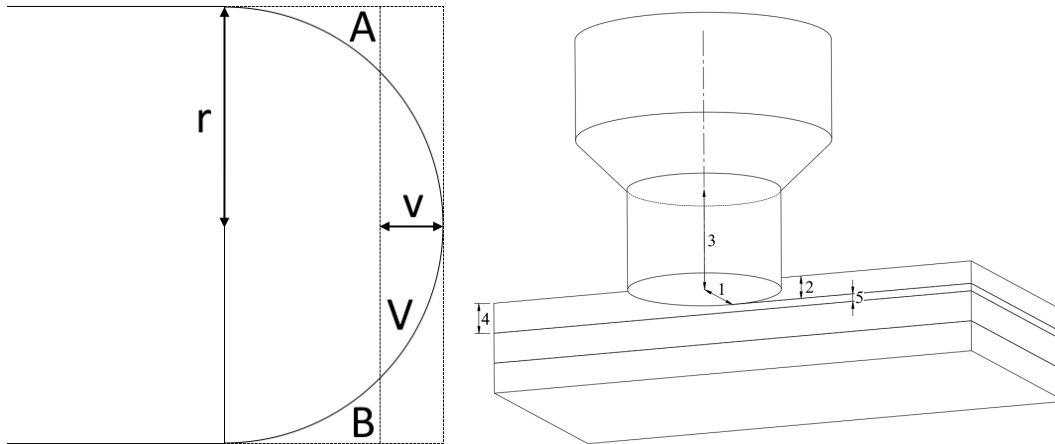
Figure 2: Schematic illustration of the necessary plastic deformation in the surface layer after deposition of each layer (left) and definition of processing parameters for the mechanical surface treatment (right) with 1 radial tool head distance, 2 axial engagement, 3 tool head length, 4 print layer height and 5 forming layer height.

Finally, the generated paths are combined with the imported G-code and exported as one G-code file. Before exporting, temperature, speeds and slip parameters can be set for the mould tool.

Based on this processing and tool concept the design for the forming tool was developed with the following aspects in mind (Figure 3):

- The forming tool must rework the part surface by local re-melting and roller burnishing. To enable re-melting, the tool head in contact with the printed object must be heated. Temperatures of up to approx. 450 °C are necessary to form the PEEK CFR 4000. Heating is provided by a high-temperature heating cartridge.
- For temperature control, thermocouples were included into the tool. A slip ring is used to realize a rotating electrical connection to the heater and thermocouple.
- In order to enable rolling as well as mechanical slip over the surface, the heated tool head must be able to actively rotate around its own axis. For this, the bearing in a statically fixed housing is necessary, which must also be able to house the stepper motor and the belt drive.
- The tool head must be interchangeable and with only minimal restrictions to the processable geometries - in this work a cylindrical head with a diameter and length of 3 mm was used.
- An integration into the existing water cooling loop as well as air cooling is used to limit temperatures and therefore thermal expansion of the bearings, preventing thermal sticking effects.

According to these specifications, the tool design has been carried out as depicted in Figure 3.
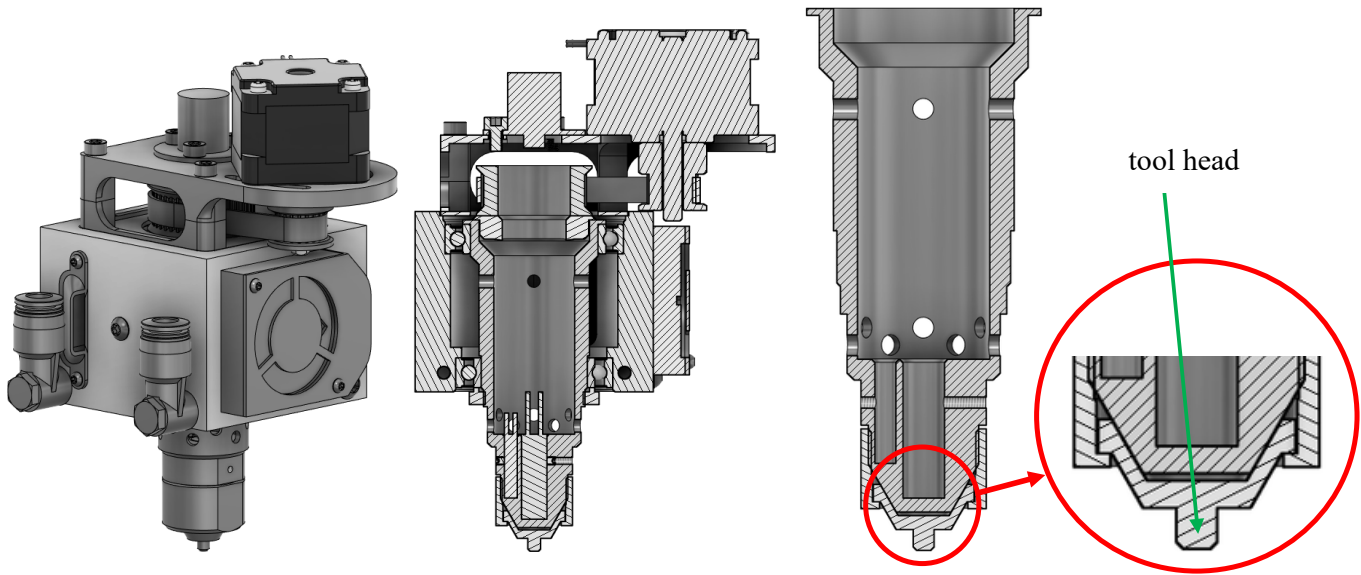
Figure 3: Images of the forming tool with the stepper motor, air cooling channels and heated rolling tool in uncut view and a cut front view with blowup of the tool. The modularity also allows for the use of the tool on other printing systems with a minimum amount of adaptation.

Surface Properties

For the determination of process-structure-property relations, variations of the relative forming layer height, the radial infeed and the mechanical slip were be investigated with the selected tool design. According to Table 2 these process parameters were varied on several levels starting from results of preliminary tests carried out with a simple heated cylinder which was linearly guided over the surface. The as build surface roughness was determined for several FFF layer heights and shows a linear correlation with the preset FFF layer height (see Figure 4 left).

Table 2: Variation of process parameters in the forming process.

Process parameter	Values
Relative forming layer height	50,100 and 800 % based on 0.3 mm printing layer height
Radial infeed	0.1 and 0.3 mm
Mechanical slip	-200 %, -100 %, 0 % and 100 %

For the mechanical slip 4 modes have been considered. During simple rolling, the tool was guided along the component surface without slippage (-100 %). Furthermore, the special case of a stationary tool (burnishing) was investigated (0 %). The last two slip values were chosen so that the tool rotates twice as fast as in the rolling case in and against the movement direction (-200 % and 200 %). For each parameter set a sample cube as described before was produced with an as-build surface state at the bottom 4 mm of the cube and a surface treated state for the rest of the sample height (see Figure 4 right).

Using the calculated radial infeed of $v \approx 0.03$ mm resulted in an inhomogeneous surface (see e.g., Figure 4 right). Not all concave regions between the printing layers could be filled and some only partially formed areas remained. Only an increase of the engagement to 0.1 mm led to a completely formed sample surface. When using the maximum forming layer height of 2.40 mm, the radial engagement had to be increased to 0.3 mm to obtain a locally closed surface.
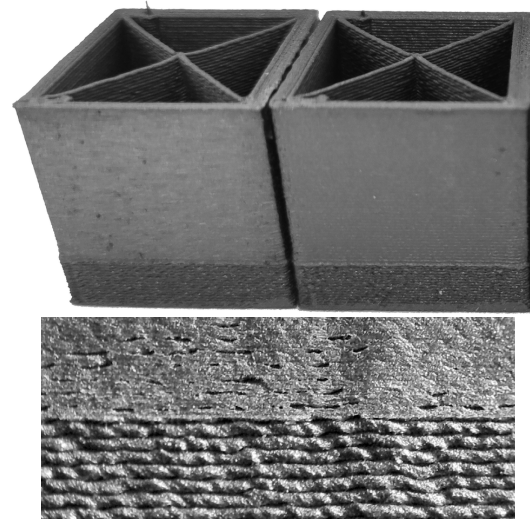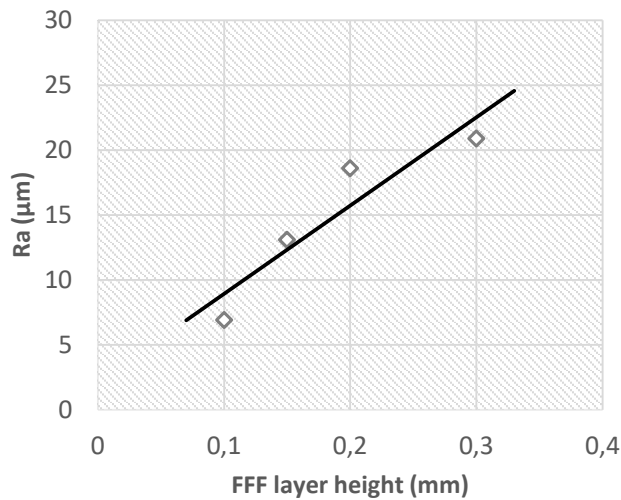
Figure 4: As-build roughness from different printing layer heights (left) and exemplary cubes from different processing parameters all showing the transition from as-build to formed surface (right). The blowup shows a transitions zone with too little radial engagement. In the upper, shaped section, concave areas can be seen which were not closed completely (right).

With respect to the surface roughness results, lower relative forming layer heights led to overall smoother surfaces. Each forming cycle produced a protrusion line at the level of the lower tool edge on the component surface. Increasing the axial contact caused the forming tool to repeatedly rework the same area. Protrusions created during the first forming could be widely reduced and disappeared through cyclic forming operations in the optimal state. By increasing the axial contact length, the result could be further improved.
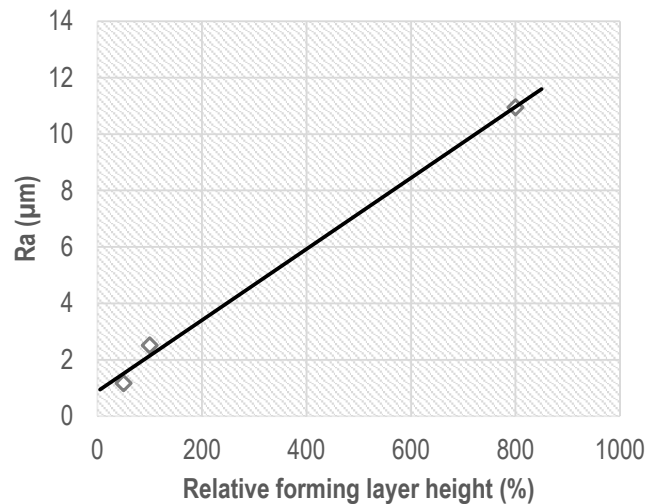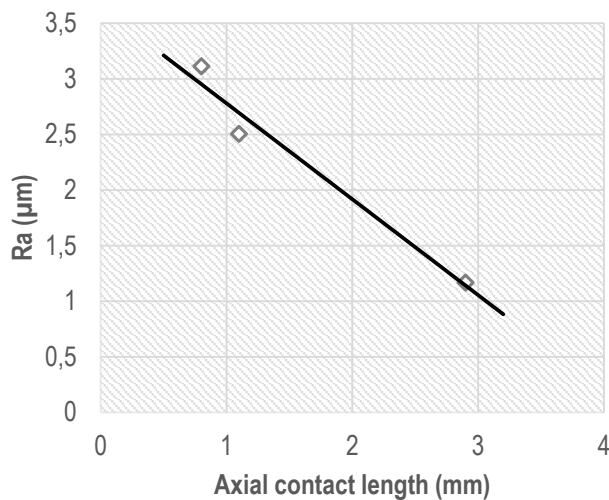
Figure 5: Dependance of the arithmetic average roughness Ra on the axial contact length (left) and the relative forming layer height (right) at respective constant complementary process parameters.

The comparison of unformed, 0.3 mm high printing layers (see Figure 4 left and Figure 5) with forming layers of the same height provides at least a 50 % reduction of the roughness values. The use of 0.15 mm high forming layers reduced the values by a factor of 10 and more in the roughness value Ra. The comparison with the finest printed 0.10 mm high layers highlights a reduction of the roughness values by a factor of at least 2. Furthermore, the existing slip between the tool and the sample surface shows no significant influence on the resulting surface roughness for each parameter configuration (see Figure 6). The direct comparison indicates higher variations of

the roughness values when the slip is changed within a sub-optimal parameter configuration while for the optimal process parameters the surface roughness stays on a constantly low value for different slip modes.
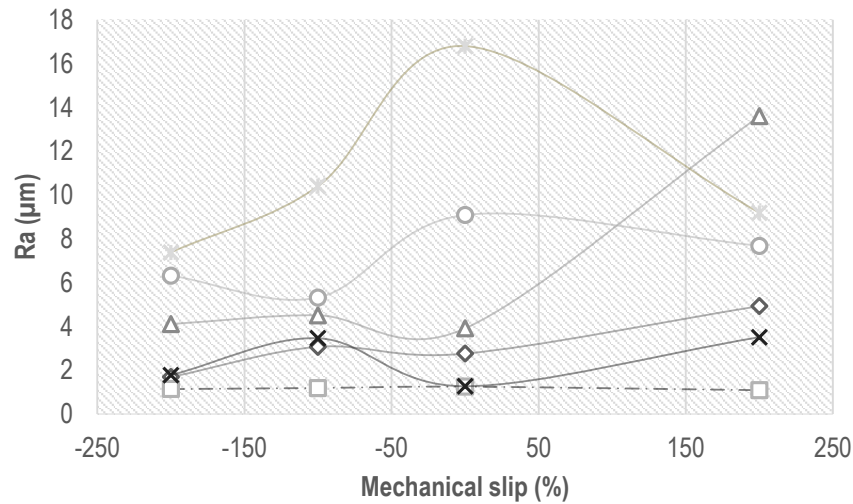
Figure 6: Influence of the mechanical slip within different process configurations. The best surface roughness independent from the mechanical slip is reached for a forming layer height of 0.15 mm (50 %), a radial infeed of 0.1 mm and an axial contact length of 2.9 mm.

The comparison and evaluation through the surface roughness show optimal results with a forming layer height of 0.15 mm (50 %), a radial infeed of 0.1 mm and an axial contact length of 2.9 mm. When forming with this combination of low forming layer height and high axial contact, the surface is reworked several times in a progressive manner. The material redistribution is divided into several passes, thus minimising the protrusion lines that are created at the tool tip.

Besides the surface roughness, an additional effect of surface densifications was expected from the mechanical surface treatment as it could already be observed from ex-situ results in metallic AM materials.
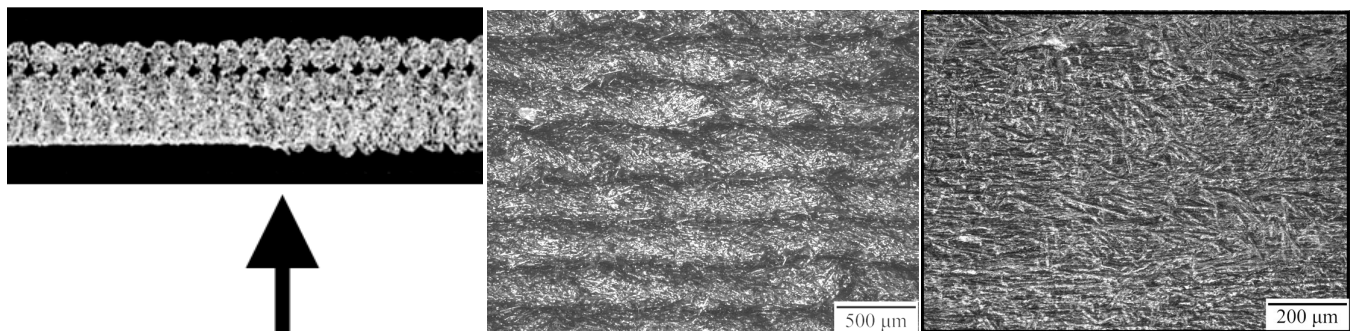
Figure 7: Slice through the Micro-CT measurement in the transitions zone between as-build and formed parts of the sample wall (left), microscopic image of the as-build surface (center) and microscopic image of the formed sample (right)

For this purpose, light optical microscopic and X-ray tomographic measurements have been evaluated in order to visualize the porosity gradients. The fiber orientation at the surface does not indicate any preferred orientation in the as-build or the formed state due to the extrusion direction or the tool path respectively. This is visible already in the light microscopic records from the clearly random fiber architecture (see Figure 7 center and right). With respect to the pores beneath the surface the visualization of a section in Figure 7 left and the 3D rendering in

Figure 8 left highlights the inter-strand pores between the perimeter strands especially in the inner perimeter. The outer perimeter shows overall less porosity and from the visualization alone a densification is hardly visible.

An evaluation of the mean gray value after segmentation of the pores and the matrix material into the depth of the sample from the surface allows for a more quantitative evaluation. The correlation to the bulk density (100 %) represented by the plateau in the center of the wall presents a more precise description of the density gradient which results in a small peak for the forming layer height of 0.15 and 0.3 mm. Furthermore, the width of the transition zone from the surface to the bulk material is smaller and the transition gradient is clearly steeper for all formed states which indicated that a higher dimensional accuracy can be reached after the surface treatment process.
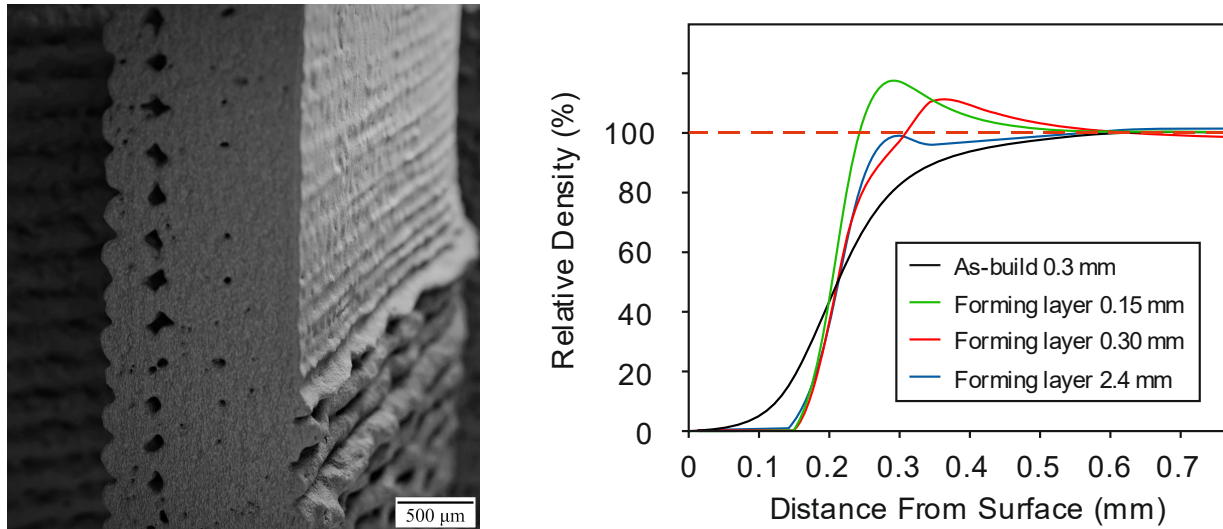
Figure 8: 3D rendering of a cut wall with process dependent porosity and surface topography (left) and curves for the relative density along the distance from the surface for different forming layer heights (right).

Discussion

The tool for print process-integrated surface finishing developed within the scope of this work proved to be functional in the first tests on simple cubes. The achievable surface finish depended significantly on the processing parameters used and reaches at least comparable results (Ra ≈ 1-1.5 μm) to machining or grinding operations used in the FFF process. Compared to other mechanical surface treatment results like peening or rolling as a post process a reduction a roughness reduction of 90 % is possible compared to 70 % mentioned in the literature. Roughness values in this range are expected to produce improvements especially in the mechanical behaviour of FFF parts. According to the measurements of the surface roughness, a low forming layer height in combination with a high axial engagement led to the smoothest surface. In practice, however, the applicability of a high axial contact is not given in every case when looking into more realistic geometries. If, in addition to vertical surfaces, surfaces inclined towards or away from the centre of the component are to be reworked, both the forming layer height and the axial contact must be minimised. In addition to inclined component surfaces, there are further geometrically determined limitations in the applicability of the mould tool. Internal corners with an angle smaller than 180° cannot be completely reworked due to the rotationally symmetrical mould geometry. Furthermore, only holes and areas that offer enough space for the forming geometry can be formed. Instead of controlling the contact pressure indirectly via the radial engagement, it seems sensible to feed back the applied force as a controlled variable. With the help of the combination of forming layer height, axial contact and measured force, the contact pressure can be controlled in a targeted manner. As part of a further technical development, the tool could be mounted on piezoelectric force sensors for this purpose.

Summary and Outlook

Within the scope of the work, a mechanical surface treatment tool was developed which allows the surfaces of FFF components to be machined in a process-integrated manner. After commissioning the first iteration of the

moulding tool in an Apium P400 FFF printer, 24 samples with different process parameter configurations out of carbon fibre reinforced Polyetheretherketone (CF-PEEK) were produced. The varied settings within the tests comprised three parameters. The forming layer height describes the distance the tool travels upwards after the entire outer contour of a component has been reworked at one height. The axial contact describes the distance in the vertical direction between the lower edge of the tool and the upper edge of the component. This indirectly determines the number or repetitions with which the tool reworks the part surface. The third parameter investigated was the slip between the tool and the component surface during finishing. These samples were then characterised with regard to their surface layer, whereby roughness measurements, light microscope images and CT images were used to analyse the surface post-processing. Specific process-structure-property relationships could be derived. As an application-oriented result components can be printed and reworked in coarser layers, which saves time. Post-processing leads to a higher surface quality and enables tighter tolerances. However, the accuracy of the manufacturing process and the required printing time pose an optimisation problem that requires component-specific trade-offs.

References

[1] D. Popescu, A. Zapciu, C. Amza, F. Baciu, R. Marinescu, FDM process parameters influence over the mechanical properties of polymer specimens: a review, Polym. Test. 69 (2018) 157–166, https://doi.org/10.1016/j.polymertesting.2018.05.020.

[2] Rodríguez-Panes, A., Claver, J., und Camacho, A. M. The influence of manufacturing parameters on the mechanical behaviour of PLA and ABS pieces manufactured by FDM: A comparative analysis. Materials, 2018. doi: 10.3390/ma11081333.

[3] Lanzotti, A., Grasso, M., Staiano, G., und Martorelli, M. The impact of process parameters on mechanical properties of parts fabricated in PLA with an open-source 3-D printer. Rapid Prototyping Journal, 2015. doi: 10.1108/RPJ-09-2014-0135.

[4] Onwubolu, G. und Rayegani, F. Characterization and optimization of mechanical properties of ABS parts manufactured by the Fused Deposition Modelling process. International Journal of Manufacturing Engineering, 2014. doi: 10.1155/2014/598531.

[5] Rankouhi, B., Javadpour, S., Delfanian, F., und Letcher, T. Failure analysis and mechanical characterization of 3D printed ABS Wwith respect to layer thickness and orientation. Journal of Failure Analysis and Prevention, 2016. doi: 10.1007/s11668-016-0113-2.

[6] Wu, W., Geng, P., Li, G., Zhao, D., Zhang, H., und Zhao, J. Influence of layer thickness and raster angle on the mechanical properties of 3D-printed PEEK and a comparative mechanical study between PEEK and ABS. Materials, 2015. doi: 10.3390/ma8095271.

[7] Rajpurohit, S. R. und Dave, H. K. Effect of process parameters on tensile strength of FDM printed PLA parts. Rapid Prototyping Journal, 2018. doi: 10.1108/RPJ-06-2017-0134.

[8] Hashmi, A. W., Mali, H. S., und Meena, A. The surface quality improvement methods for FDM printed parts: a review. Springer International Publishing, 2021. doi: 10.1007/978-3-030-68024-4_9.

[9] Chohan, J. S. und Singh, R. Pre and post processing techniques to improve surface characteristics of FDM parts: a state of art review and future applications. Rapid Prototyping Journal, 2017. doi: 10.1108/RPJ-05-2015-0059.

[10] Chueca de Bruijn, A., Gómez-Gras, G., & Pérez, M. A. (2021). A comparative analysis of chemical, thermal, and mechanical post-process of fused filament fabricated polyetherimide parts for surface quality enhancement. Materials, 14(19), 5880.

[11] Mwema, F. M. und Akinlabi, E. T. Surface engineering strategy. Springer International Publishing, 2020. doi:10.1007/978-3-030-48259-6_4.

[12] Kanger, C., Hadidi, H., Akula, S., Sandman, C., Quint, J., Alsunni, M., ... & Sealy, M. P. (2017). Effect of process parameters and shot peening on mechanical behavior of ABS parts manufactured by fused filament fabrication (FFF). In 2017 International Solid Freeform Fabrication Symposium. University of Texas at Austin.

[13] Singh, R. und Singh, M. Surface roughness improvement of cast components in vacuum moulding by intermediate barrel finishing of Fused Deposition Modelling patterns. Proceedings of the Institution of Mechanical Engineers, Part E: Journal of Process Mechanical Engineering, 2017. doi:10.1177/0954408915595576.

[14] de Bruijn, A. C., Gómez-Gras, G., & Pérez, M. A. (2021). On the effect upon the surface finish and mechanical performance of ball burnishing process on fused filament fabricated parts. *Additive Manufacturing*, *46*, 102133.

[15] Lalehpour, A., Janeteas, C., und Barari, A. Surface roughness of FDM parts after postprocessing with acetone vapor bath smoothing process. The International Journal of Advanced Manufacturing Technology, 2017. doi:10.1007/s00170-017-1165-5.

[16] Taufik, M. und Jain, P. K. Laser assisted finishing process for improved surface finish of Fused Deposition Modelled parts. Journal of Manufacturing Processes, 2017. doi:10.1016/j.jmapro.2017.09.020.

[17] Kuczko, W., Górski, F., Wichniarek, R., und Buń, P. Influence of post-processing on accuracy of FDM products. Advances in Science and Technology Research Journal, 2017. doi:10.12913/22998624/70996.